Lightest scalar and tensor resonances in $\gamma\gamma \to \pi\pi$ after the Belle experiment

N. N. Achasov* and G. N. Shestakov+

Laboratory of Theoretical Physics, S.L. Sobolev Institute for Mathematics, 630090, Novosibirsk, Russia

(Received 7 December 2007; published 25 April 2008)

New high statistics Belle data on the $\gamma\gamma \to \pi^+\pi^-$ reaction cross section measured in the range of pion-pair invariant masses $\sqrt{s}$ between 0.8 GeV and 1.5 GeV are analyzed to clarify the current situation around the $\sigma(600)$, $f_0(980)$, and $f_2(1270)$ resonances in $\gamma\gamma$ collisions. The present analysis shows that the direct coupling constants of the $\sigma(600)$ and $f_0(980)$ resonances to $\gamma\gamma$ are small, and the $\sigma(600) \to \gamma\gamma$ and $f_0(980) \to \gamma\gamma$ decays are four-quark transitions caused by the $\pi^+\pi^-$ and K^+K^- loop mechanisms, respectively. The chiral shielding of the $\sigma(600)$ resonance takes place in the reactions $\gamma\gamma \to \pi\pi$ as well as in $\pi\pi$ scattering. Some results of a simultaneous description of the $\gamma\gamma \to \pi^+\pi^-$ and $\gamma\gamma \to \pi^0\pi^0$ Belle data are also presented. In particular, the following tentative estimate of the $f_2(1270) \to \gamma\gamma$ decay width is obtained: $\Gamma_{f_2\to\gamma\gamma}(m^2_{f_2}) \approx 3.68$ keV.

DOI: 10.1103/PhysRevD.77.074020 PACS numbers: 12.39.−x, 13.40.−f, 13.75.Lb

I. INTRODUCTION

Recently, the Belle Collaboration performed precise measurements of the $\gamma\gamma \to \pi^+\pi^-$ reaction cross section for pion-pair invariant masses $\sqrt{s}$ ranging from 0.8 to 1.5 GeV [1,2]. Owing to the huge statistics and good energy resolution, a clear signal from the $f_0(980)$ resonance was first discovered with the Belle detector. Evidences for the $f_0(980)$ production in $\gamma\gamma$ collisions obtained in a series of previous measurements [3–8] were essentially less conclusive. The $f_0(980)$ signal observed in the Belle experiment turned out to be rather small. This feature is in good qualitative agreement with the prediction of the four-quark model [9]. A detailed analysis of the preliminary Belle data [1] in the $f_0(980)$ region was performed in Ref. [10]. In particular, it was found [10] that the magnitude and shape of the $f_0(980)$ peak observed in the $\gamma\gamma \to \pi^+\pi^-$ reaction cross section excellently agree with the K^+K^- loop mechanism of the $f_0(980)$ production, $\gamma\gamma \to K^+K^- \to f_0(980) \to \pi^+\pi^-$. This result is one of many in favor of the four-quark nature of the $f_0(980)$ state [11,12].

In this paper we clarify the current situation around the $\sigma(600)$, $f_0(980)$, and $f_2(1270)$ resonances in the reactions $\gamma\gamma \to \pi\pi$ by analyzing the final Belle data [2] on the $\gamma\gamma \to \pi^+\pi^-$ cross section in the region $0.8 \le \sqrt{s} \le 1.5$ GeV, together with the Crystal Ball data [3,7] on the reaction $\gamma\gamma \to \pi^0\pi^0$ for $2m_\pi < \sqrt{s} < 1.6$ GeV. As the first step, in Sec. II, the pure Born cross sections and those involving the S wave Born contributions modified by strong final-state interactions are compared with the available data on the reactions $\gamma\gamma \to \pi\pi$ [2–4,6,7]. Such a comparison is very useful because it enables us to gain some idea of the scope and shape of other possible contributions to the cross sections. The scheme taking into account the S wave final-state interactions between pions and kaons, in which the $\sigma(600)$ and $f_0(980)$ resonances take part, is presented in Sec. III. In this scheme we essentially use the results of the simultaneous analysis of the data on the $\phi \to \pi^0\pi^0\gamma$ decay, $\pi\pi$ scattering, and reaction $\pi\pi \to K\bar{K}$ [13], as well as the results of the previous analyses of the $\gamma\gamma \to \pi\pi$ reaction mechanisms [10,14]. In Secs. IV and V, tentative values of the direct coupling constants of the $\sigma(600)$ and $f_0(980)$ resonances to $\gamma\gamma$ are determined from the Belle and Crystal Ball data. It is important that these constants turn out to be small, and consequently, the $\sigma(600) \to \gamma\gamma$ and $f_0(980) \to \gamma\gamma$ decays are, in fact, the four-quark transitions caused by the $\pi^+\pi^-$ and K^+K^- loop mechanisms, respectively. The chiral shielding of the $\sigma(600)$ resonance takes place in the reactions $\gamma\gamma \to \pi\pi$ [14] as well as in $\pi\pi$ scattering [11–13,15]. In addition, in Sec. V, we make some comments on the difficulties of interpreting the experimental measurements for $\gamma\gamma \to \pi^0\pi^0$ production in the $f_2(1270)$ resonance region. Here we also point to a possible way out and announce some preliminary results of a simultaneous description of the $\gamma\gamma \to \pi^+\pi^-$ data and the latest, very high statistics Belle data on the $\gamma\gamma \to \pi^0\pi^0$ reaction cross section. The estimates for the $f_2(1270) \to \gamma\gamma$ decay width are also given. Conclusions are shortly formulated in Sec. VI.

II. DATA ON $\gamma\gamma \to \pi\pi$ AND THE BORN CONTRIBUTIONS

The Mark II [4], CELLO [6], and Belle [2,16] data on the cross section for the reaction $\gamma\gamma \to \pi^+\pi^-$ are shown in Fig. 1(a). All the data correspond to a limited angular range of the registration of the charged pions, such that $|\cos\theta| \le 0.6$, where θ is the polar angle of the produced $\pi^\pm$ meson in the center-of-mass system of two initial photons. The Belle data are represented with statistical errors only, the relative values of which are approximately

*achasov@math.nsc.ru
+shestako@math.nsc.ru

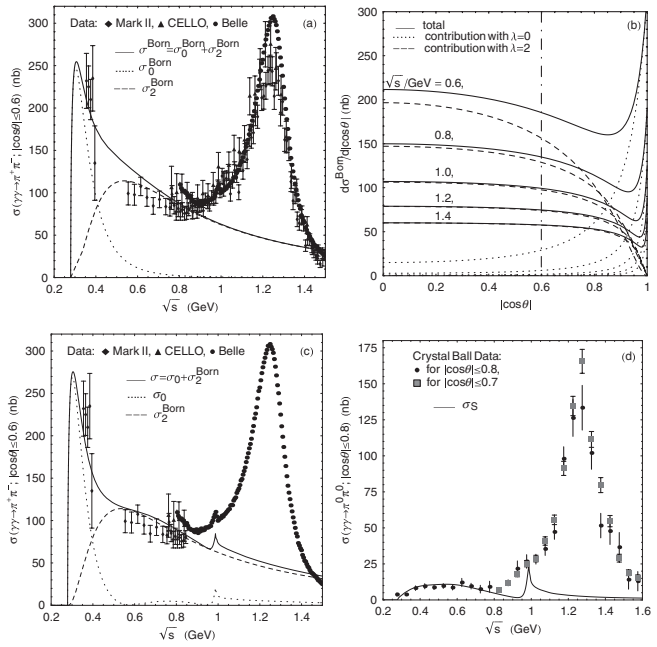

FIG. 1. The data from Mark II [3], CELLO [6], and Belle [2,16] on the cross section for $\gamma\gamma \to \pi^+\pi^-$, and from Crystal Ball [4,7] on the cross section for $\gamma\gamma \to \pi^0\pi^0$. The theoretical curves correspond to the pure Born cross sections, as well as the Born cross sections modified for strong final-state interactions in the S wave. See the text for details.

equal to 0.5%–1.5%. The $\sqrt{s}$ bin size in the Belle experiment has been chosen to be 5 MeV, with the mass resolution of about 2 MeV.

Figure 1(a) also represents the comparison between the data and theoretical curves corresponding to the pure Born cross sections for the process $\gamma\gamma \to \pi^+\pi^-$ for $|\cos\theta| \leq 0.6$: the total integrated cross section $\sigma^{\rm Born}$ and the integrated cross sections $\sigma_\lambda^{\rm Born}$, where $\lambda = 0$ or 2 is the absolute value of the photon helicity difference. According to the Low theorem, the Born contributions give the exact physical amplitude of the crossing reaction $\gamma\pi^\pm \to \gamma\pi^\pm$ near its threshold. If strong interactions of pions near the $\pi\pi$ threshold are not too large (this is the case owing to chiral symmetry), then the Born contributions have to dominate near the threshold of the reaction $\gamma\gamma \to \pi^+\pi^-$ as well. As is seen from Fig. 1(a), this expectation does not contradict the data existing in the threshold region, though their errors are very large as yet. Moreover, the Born amplitudes can be used as a quite reasonable approximation of the primary background (nonresonance) contributions in the reaction $\gamma\gamma \to \pi^+\pi^-$ up to the $f_2(1270)$ resonance region, as well as a reasonable foundation for constructing the amplitudes involving the strong final-state interactions; see, for example, [10,14,17–21]. The pure Born contributions have the following features. First, $\sigma^{\rm Born}$ reaches its maximum at $\sqrt{s} \approx 0.3$ GeV, in the vicinity of which $\sigma^{\rm Born} \approx \sigma_0^{\rm Born}$. However, $\sigma_0^{\rm Born}$ involving the S wave contribution decreases rapidly with increasing $\sqrt{s}$ so that $\sigma^{\rm Born}$ is fully dominated by the contribution from $\sigma_2^{\rm Born}$ for $\sqrt{s} > 0.5$ GeV; see Fig. 1(a). Second, though $\sigma_2^{\rm Born}$ is determined essentially by the D wave contribution with $\lambda = 2$, the differential cross section $d\sigma^{\rm Born}/d|\cos\theta|$ in the region $|\cos\theta| \leq 0.6$ changes very weakly (see Fig. 1 (b)), and it becomes more and more flat in this region of $|\cos\theta|$ as $\sqrt{s}$ increases. Therefore, in analyzing the data corresponding to this angular range, one should be very careful to make a definite conclusion about the partial wave structure of the smooth background. In other words, the above example hints that the assumption of the S wave dominance [16] may be completely unjustified in reality.

Figure 1(c) shows only the Belle data in the region $\sqrt{s} > 0.85$ to illustrate clearly the discovered signal from the $f_0(980)$ resonance. The visible height of the $f_0(980)$ peak is of about 15 nb over the overall smooth background of the order of 100 nb, and its visible (effective) width is of about 30–35 MeV. It is natural to consider that the large background under the $f_0(980)$ resonance is mainly caused by the contributions from the Born amplitude with $\lambda = 2$ and the $f_2(1270)$ resonance production amplitude also with $\lambda = 2$. Figure 1(c) shows the theoretical curves for the total integrated cross section $\sigma = \sigma_0 + \sigma_2^{\rm Born}$ and the integrated ones σ_0 and $\sigma_2^{\rm Born}$. Here σ_0 is the $\gamma\gamma \to \pi^+\pi^-$ cross section with $\lambda = 0$ in which the contributions of the S wave Born amplitude are modified by the strong final-state interactions. All the higher partial waves, D, G, etc., in σ_0 are taken in the Born approximation [10]. The above modification leads to a signal from the $f_0(980)$ resonance in σ_0 whose magnitude and shape are in surprising agreement with the Belle data; see Fig. 1(c). An explicit form for σ_0 will be given below. The comparison of the curves in Figs. 1(a) and 1(c) shows that the S wave contribution to $\sigma(\gamma\gamma \to \pi^+\pi^-; |\cos\theta| \leq 0.6)$ is small for $\sqrt{s} > 0.5$ in any case. Certainly, the $f_2(1270)$ resonance contribution is an important component needed for the description of the Belle data in the whole region of $\sqrt{s}$ from 0.8 to 1.5 GeV.

The incorporation of final-state interactions in the S wave Born amplitude $\gamma\gamma \to \pi^+\pi^-$ leads to a striking prediction for the S wave amplitude $\gamma\gamma \to \pi^0\pi^0$ [10]. Figure 1(d) demonstrates the comparison of the S wave partial cross section for the reaction $\gamma\gamma \to \pi^0\pi^0$, σ_S, calculated in the way outlined above, with the Crystal Ball data [4,7]. Since σ_S does not contain any fitting parameter, the agreement with experiment in the region $2m_\pi \leq \sqrt{s} \leq 0.8$ GeV is quite reasonable. Note that, in the Crystal Ball experiments [4,7], the $\gamma\gamma \to \pi^0\pi^0$ cross section was scanned with a 50-MeV-wide step, and therefore the narrow $f_0(980)$ structure could not be resolved. It is also clear that in the reaction $\gamma\gamma \to \pi^0\pi^0$, as well as in $\gamma\gamma \to \pi^+\pi^-$, the $f_2(1270)$ resonance manifestation domain begins for $\sqrt{s} > 0.8$ GeV. The latest, high statistics Belle data on the $\gamma\gamma \to \pi^0\pi^0$ reaction cross section in the

region $0.73 < \sqrt{s} < 1.5$ GeV are presented and discussed below in Sec. V.

III. S WAVE FINAL-STATE INTERACTIONS

In the field theory approach, one has the following S wave $\gamma\gamma \to \pi\pi$ amplitudes, satisfying the unitarity condition and involving the electromagnetic Born contributions "dressed" (modified) by strong final-state interactions [10,14,17,22],

$$\begin{aligned} M_S(\gamma\gamma \to \pi^+\pi^-; s) &= M_S^{\rm Born}(s) + 8\alpha I_{\pi^+\pi^-}(s) T_{\pi^+\pi^- \to \pi^+\pi^-}(s) + 8\alpha I_{K^+K^-}(s) T_{K^+K^- \to \pi^+\pi^-}(s) \\ &= (\text{for } 2m_\pi \le \sqrt{s} \le 2m_K) \\ &= \frac{2}{3} e^{i\delta_0^0(s)} \left\{ M_S^{\rm Born}(s) \cos\delta_0^0(s) + \frac{8\alpha}{\rho_{\pi^+}(s)} \,{\rm Re}[I_{\pi^+\pi^-}(s)] \sin\delta_0^0(s) \pm 12\alpha I_{K^+K^-}(s) |T_{K^+K^- \to \pi^+\pi^-}(s)| \right\} \\ &\quad + \frac{1}{3} e^{i\delta_0^2(s)} \left\{ M_S^{\rm Born}(s) \cos\delta_0^2(s) + \frac{8\alpha}{\rho_{\pi^+}(s)} \,{\rm Re}[I_{\pi^+\pi^-}(s)] \sin\delta_0^2(s) \right\}, \end{aligned} \tag{1}$$

$$\begin{aligned} M_S(\gamma\gamma \to \pi^0\pi^0; s) &= 8\alpha I_{\pi^+\pi^-}(s) T_{\pi^+\pi^- \to \pi^0\pi^0}(s) + 8\alpha I_{K^+K^-}(s) T_{K^+K^- \to \pi^0\pi^0}(s) \\ &= (\text{for } 2m_\pi \le \sqrt{s} \le 2m_K) \\ &= \frac{2}{3} e^{i\delta_0^0(s)} \left\{ M_S^{\rm Born}(s) \cos\delta_0^0(s) + \frac{8\alpha}{\rho_{\pi^+}(s)} \,{\rm Re}[I_{\pi^+\pi^-}(s)] \sin\delta_0^0(s) \pm 12\alpha I_{K^+K^-}(s) |T_{K^+K^- \to \pi^0\pi^0}(s)| \right\} \\ &\quad - \frac{2}{3} e^{i\delta_0^2(s)} \left\{ M_S^{\rm Born}(s) \cos\delta_0^2(s) + \frac{8\alpha}{\rho_{\pi^+}(s)} \,{\rm Re}[I_{\pi^+\pi^-}(s)] \sin\delta_0^2(s) \right\}, \end{aligned} \tag{2}$$

where $M_S^{\rm Born}(s)$ is the S wave Born amplitude of the process $\gamma\gamma \to \pi^+\pi^-$; for $s \ge 4m_{\pi^+}^2$,

$$\begin{aligned} M_S^{\rm Born}(s) &= \frac{16\pi\alpha m_{\pi^+}^2}{s\rho_{\pi^+}(s)} \ln\frac{1+\rho_{\pi^+}(s)}{1-\rho_{\pi^+}(s)} \\ &= \frac{8\alpha}{\rho_{\pi^+}(s)} \,{\rm Im} I_{\pi^+\pi^-}(s), \end{aligned} \tag{3}$$

$\rho_{\pi^+}(s) = (1 - 4m_{\pi^+}^2/s)^{1/2}$, $\delta_0^0(s)$ and $\delta_0^2(s)$ are the phase shifts of the S wave $\pi\pi$ scattering amplitudes with isospin $I = 0$ and 2, respectively (see below for details), and $\alpha = 1/137$. The second equalities in Eqs. (1) and (2) are valid just in the elastic region, practically for $2m_\pi \le \sqrt{s} \le 2m_K$, and clearly demonstrate the fulfillment of the Watson theorem for the S wave $\gamma\gamma \to \pi\pi$ amplitudes with definite isospin. The function $I_{K^+K^-}(s)$ is given by

$$I_{K^+K^-}(s) = \begin{cases} \frac{m_{K^+}^2}{s}\left[\pi + i\ln\frac{1+\rho_{K^+}(s)}{1-\rho_{K^+}(s)}\right]^2 - 1, & s \ge 4m_{K^+}^2, \\ \frac{m_{K^+}^2}{s}\left[\pi - 2\arctan|\rho_{K^+}(s)|\right]^2 - 1, & 0 \le s \le 4m_{K^+}^2, \end{cases} \tag{4}$$

$\rho_{K^+}(s) = (1 - 4m_{K^+}^2/s)^{1/2}$ for $s \ge 4m_{K^+}^2$ and $\rho_{K^+}(s) \to i|\rho_{K^+}(s)|$ if $0 \le s \le 4m_{K^+}^2$. $I_{\pi^+\pi^-}(s)$ results from $I_{K^+K^-}(s)$ by replacing m_{K^+} and $\rho_{K^+}(s)$ by m_{π^+} and $\rho_{\pi^+}(s)$, respectively. Finally, $T_{\pi^+\pi^- \to \pi^+\pi^-}(s)$, $T_{\pi^+\pi^- \to \pi^0\pi^0}(s)$, and $T_{K^+K^- \to \pi^+\pi^-}(s) = T_{K^+K^- \to \pi^0\pi^0}(s)$ are the S wave amplitudes of hadronic reactions indicated in their subscripts. Equations (1) and (2) assume that the amplitudes $T_{\pi^+\pi^- \to \pi\pi}(s)$ and $T_{K^+K^- \to \pi\pi}(s)$ lie on the mass shell in the rescattering loops $\gamma\gamma \to \pi^+\pi^- \to \pi\pi$ and $\gamma\gamma \to K^+K^- \to \pi\pi$. The functions $I_{\pi^+\pi^-}(s)$ and $I_{K^+K^-}(s)$ are the attributes of the triangle diagrams $\gamma\gamma \to \pi^+\pi^- \to \sigma$, f_0 and $\gamma\gamma \to K^+K^- \to \sigma$, f_0 (or any other scalars). Thus, the amplitudes in Eqs. (1) and (2) represent the S wave $\gamma\gamma \to \pi^+\pi^-$ and $\gamma\gamma \to K^+K^-$ Born contributions modified by the strong elastic and inelastic final-state interactions.

The helicity-0 cross section integrated over the range $|\cos\theta| \le Z_0 < 1$ and involving the amplitude $M_S(\gamma\gamma \to \pi^+\pi^-; s)$ and the pure Born higher partial wave amplitudes can be written in the form

$$\begin{aligned} &\sigma_{\lambda=0}(\gamma\gamma \to \pi^+\pi^-, |\cos\theta| \le Z_0) \\ &\quad = \frac{\rho_{\pi^+}(s)}{32\pi s}\left\{ Z_0 |\tilde{A}_S(s)|^2 + C\,{\rm Re}[\tilde{A}_S(s)] \frac{1}{\rho_{\pi^+}(s)} \right. \\ &\qquad \times \ln\frac{1+Z_0\rho_{\pi^+}(s)}{1-Z_0\rho_{\pi^+}(s)} + C^2\left[\frac{Z_0/2}{1-Z_0^2\rho_{\pi^+}^2(s)} \right. \\ &\qquad \left.\left. + \frac{1}{4\rho_{\pi^+}(s)} \ln\frac{1+Z_0\rho_{\pi^+}(s)}{1-Z_0\rho_{\pi^+}(s)} \right] \right\}, \end{aligned} \tag{5}$$

where $\tilde{A}_S(s) = M_S(\gamma\gamma \to \pi^+\pi^-; s) - M_S^{\rm Born}(s)$ [see Eq. (1)] and $C = 32\pi\alpha m_{\pi^+}^2/s$. The cross section σ_0, shown, for example, in Fig. 1(c) by the dotted curve (see also the solid curve in this figure and the next section for details), is given by

$$\sigma_0 = \sigma_{\lambda=0}(\gamma\gamma \to \pi^+\pi^-, |\cos\theta| \le 0.6). \tag{6}$$

Similarly, the S wave cross section for the reaction $\gamma\gamma \to \pi^0\pi^0$ is given by

$$\sigma_S(\gamma\gamma \to \pi^0\pi^0) = \frac{\rho_{\pi^+}(s)}{64\pi s}|M_S(\gamma\gamma \to \pi^0\pi^0; s)|^2; \quad (7)$$

see Eq. (2). The cross section σ_S shown in Fig. 1(d) corresponds to $0.8\sigma_S(\gamma\gamma \to \pi^0\pi^0)$.

To construct σ_0 and σ_S, the amplitudes $T_{\pi^+\pi^-\to\pi^+\pi^-}(s)$, $T_{\pi^+\pi^-\to\pi^0\pi^0}(s)$, and $T_{K^+K^-\to\pi^+\pi^-}(s) = T_{\pi^+\pi^-\to K^+K^-}(s)$ need to be known. They are related to the S wave $\pi\pi$ scattering amplitude $T_0^I(s)$, the phase shift $\delta_0^I(s)$, and inelasticity $\eta_0^I(s)$ with definite isospin $I = 0$, 2 in the conventional way:

$$\begin{aligned} T_{\pi^+\pi^-\to\pi^+\pi^-}(s) &= [2T_0^0(s) + T_0^2(s)]/3, \\ T_{\pi^+\pi^-\to\pi^0\pi^0}(s) &= 2[T_0^0(s) - T_0^2(s)]/3, \end{aligned} \quad (8)$$

$$T_0^I(s) = \{\eta_0^I(s)\exp[2i\delta_0^I(s)] - 1\}/[2i\rho_{\pi^+}(s)], \quad (9)$$

$$\eta_0^0(s) = \sqrt{1 - 4\rho_{K^+}\rho_{\pi^+}(3/2)|T_{\pi^+\pi^-\to K^+K^-}(s)|^2\theta(s - 4m_{K^+}^2)} - \ldots. \quad (10)$$

Dots in $\eta_0^0(s)$ denote the contributions from other inelastic channels $\pi^+\pi^- \to K^0\bar{K}^0$, $\pi^+\pi^- \to \eta\eta$, etc. For $4m_\pi^2 \le s \le 4m_K^2$, the amplitude $T_{\pi^+\pi^-\to K^+K^-}(s) = \pm e^{i\delta_0^0(s)} \times |T_{\pi^+\pi^-\to K^+K^-}(s)|$ for the 4π channel contribution is small [10,13]. Note that the plus sign is realized here according to Ref. [13]. We also set $\eta_0^2(s) = 1$ for all s of interest.

A parametrization of the amplitudes $T_0^0(s)$ and $T_{K^+K^-\to\pi^+\pi^-}(s)$ has been thoroughly described in Ref. [13]. It has been used for the simultaneous analysis of the data on the $\pi^0\pi^0$ mass distribution in the $\phi \to \pi^0\pi^0\gamma$ decay, $\pi\pi$ scattering in the region $2m_\pi \le \sqrt{s} < 1.6$ GeV, and the reaction $\pi\pi \to K\bar{K}$ [13]. The key idea of this parametrization is that the amplitude $T_0^0(s)$ incorporates the contributions from the mixed $\sigma(600)$ and $f_0(980)$ resonances and from the nonresonant background having a large negative phase which hides the $\sigma(600)$ meson [11–13]. Originally, the presence of such a background in $\pi\pi$ scattering was established in the linear σ model [15]. It has been made clear that shielding of wide, lightest scalar mesons in chiral dynamics is very natural. As for $\gamma\gamma$ interactions, Eqs. (1) and (2) transfer the chiral shielding effect of the $\sigma(600)$ from $\pi\pi$ scattering to the $\gamma\gamma \to \pi\pi$ reaction amplitudes [14]. The shielding of the σ meson takes place in the $\gamma\gamma \to \pi\pi$ amplitudes for the strong destructive interference between the resonance and background contributions as in the $\pi\pi \to \pi\pi$ amplitudes. This was first demonstrated in the frame of the $SU_L(2) \times SU_R(2)$ linear σ model in Ref. [14]. If such a shielding was absent, then the cross section σ_S would reach approximately 100 nb just above the $\pi^0\pi^0$ threshold, owing to the $\pi^+\pi^-$ loop mechanism of the $\sigma(600) \to \gamma\gamma$ decay [14], instead of about 10 nb as in experiment [see Fig. 1(d)].

We now return to the parametrization of the strong amplitudes. In terms of the mixed $\sigma(600)$ and $f_0(980)$ resonances and the necessary background contributions, the explicit form of the amplitudes $T_0^0(s)$ and $T_{K^+K^-\to\pi^+\pi^-}(s)$ is given by [13]

$$T_0^0(s) = \frac{\eta_0^0(s)e^{2i\delta_0^0(s)} - 1}{2i\rho_{\pi^+}(s)} = T_B^{\pi\pi}(s) + e^{2i\delta_B^{\pi\pi}(s)}T_{\rm res}^{\pi\pi}(s), \quad (11)$$

$$T_{K^+K^-\to\pi^+\pi^-}(s) = e^{i[\delta_B^{\pi\pi}(s) + \delta_B^{K\bar{K}}(s)]}T_{\rm res}^{K^+K^-\to\pi^+\pi^-}(s), \quad (12)$$

where $\delta_B^{\pi\pi}(s)$ and $\delta_B^{K\bar{K}}(s)$ are the phases of the elastic background in the $I = 0$ S wave $\pi\pi$ and $K\bar{K}$ channels, respectively, $T_B^{\pi\pi}(s) = \{\exp[2i\delta_B^{\pi\pi}(s)] - 1\}/[2i\rho_{\pi^+}(s)]$ is the $I = 0$ S wave $\pi\pi$ background amplitude, the amplitudes of the $\sigma(600) - f_0(980)$ resonance complex are

$$\begin{aligned} T_{\rm res}^{\pi\pi}(s) &= \frac{\eta_0^0(s)e^{2i\delta_{\rm res}(s)} - 1}{2i\rho_{\pi^+}(s)} \\ &= \frac{3}{32\pi}\frac{g_{\sigma\pi^+\pi^-}[D_{f_0}(s)g_{\sigma\pi^+\pi^-} + \Pi_{f_0\sigma}(s)g_{f_0\pi^+\pi^-}] + g_{f_0\pi^+\pi^-}[D_\sigma(s)g_{f_0\pi^+\pi^-} + \Pi_{f_0\sigma}(s)g_{\sigma\pi^+\pi^-}]}{D_\sigma(s)D_{f_0}(s) - \Pi_{f_0\sigma}^2(s)}, \end{aligned} \quad (13)$$

and

$$T_{\rm res}^{K^+K^-\to\pi^+\pi^-}(s) = \frac{1}{16\pi}\frac{g_{\sigma K^+K^-}[D_{f_0}(s)g_{\sigma\pi^+\pi^-} + \Pi_{f_0\sigma}(s)g_{f_0\pi^+\pi^-}] + g_{f_0K^+K^-}[D_\sigma(s)g_{f_0\pi^+\pi^-} + \Pi_{f_0\sigma}(s)g_{\sigma\pi^+\pi^-}]}{D_\sigma(s)D_{f_0}(s) - \Pi_{f_0\sigma}^2(s)}, \quad (14)$$

and the phase shift $\delta_0^0(s) = \delta_B^{\pi\pi}(s) + \delta_{\rm res}(s)$. We use for $\delta_B^{\pi\pi}(s)$, for propagators of the $\sigma(600)$ and $f_0(980)$ resonances $1/D_\sigma(s)$ and $1/D_{f_0}(s)$, and for the nondiagonal matrix element of the polarization operator $\Pi_{f_0\sigma}(s)$, the expressions presented in Ref. [13] (see also Ref. [23]). In the accepted normalization the relation between the coupling constant $g_{\sigma\pi^+\pi^-}$ and the corresponding partial decay width of the $\sigma(600)$ is given by $\Gamma_{\sigma\to\pi\pi}(s) = [3g_{\sigma\pi^+\pi^-}^2/(32\pi)]\rho_{\pi^+}(s)$. Similar relations take place for the $\sigma(600)$ decays into $K\bar{K}$, $\eta\eta$, $\eta\eta'$, and $\eta'\eta'$, and for the

$f_0(980)$ decays into $\pi\pi$, $K\bar{K}$, $\eta\eta$, $\eta\eta'$, and $\eta'\eta'$. Remember that the $\sigma(600)$ couples mainly to $\pi\pi$, $\eta\eta$, $\eta\eta'$, and $\eta'\eta'$, and the $f_0(980)$ to $K\bar{K}$, $\eta\eta$, $\eta\eta'$, and $\eta'\eta'$ [13].

The various fits corresponding to the different values of the parameters in the strong amplitudes have been considered in Ref. [13]. All of these fits give excellent descriptions of a large set of the data on the $\phi \to \pi^0\pi^0\gamma$ decay, $\delta_0^0(s)$, and $\eta_0^0(s)$. The curves for σ_0 and σ in Fig. 1(c), and for σ_S in Fig. 1(d), calculated with the use of Eqs. (1), (2), (5), and (7), correspond to fit 1 from Table I presented in Ref. [13]; see also Ref. [24]. For the phase shift $\delta_0^2(s)$, we take the parametrization of Ref. [25].

According to Eqs. (1) and (2), the $\sigma(600) \to \gamma\gamma$ and $f_0(980) \to \gamma\gamma$ decays are described by the $\pi^+\pi^-$ and K^+K^- loop diagrams, Resonances $\to (\pi^+\pi^-, K^+K^-) \to \gamma\gamma[I_{\pi^+\pi^-}(s), I_{K^+K^-}(s)]$. Consequently, they are the four-quark transitions [14]. Let us emphasize that there are no free parameters specific for the reactions $\gamma\gamma \to \pi\pi$ in Eqs. (1) and (2), and that the existing data are not indicative of the necessity of introducing such parameters. Nevertheless, in the next section we shall supplement Eqs. (1) and (2) with the terms involving unknown direct coupling constants of the $\sigma(600)$ and $f_0(980)$ resonances to $\gamma\gamma$, and we shall attempt to extract the values of these undoubtedly important physical characteristics from the data. Note that some evidence for smallness of these constants was obtained previously in Refs. [10,14] within the more simple models for the amplitudes $\gamma\gamma \to \pi\pi$. Later, a similar conclusion about the direct coupling of the $\sigma(600)$ to $\gamma\gamma$ was also obtained in Ref. [26].

IV. DIRECT COUPLINGS OF THE $\sigma(600)$ AND $f_0(980)$ TO $\gamma\gamma$

We now add to the right-hand side of Eq. (1) the amplitude $M_{\rm res}^{\rm direct}(\gamma\gamma \to \pi^+\pi^-; s)$ caused by the contribution from the mixed $\sigma(600)$ and $f_0(980)$ resonances [13] with the direct coupling constants of the $\sigma(600)$ and $f_0(980)$ to photons, $g^{(0)}_{\sigma\gamma\gamma}$ and $g^{(0)}_{f_0\gamma\gamma}$,

$$M_{\rm res}^{\rm direct}(\gamma\gamma \to \pi^+\pi^-; s) = s e^{i\delta_B^{\pi\pi}(s)} \frac{g^{(0)}_{\sigma\gamma\gamma}[D_{f_0}(s) g_{\sigma\pi^+\pi^-} + \Pi_{f_0\sigma}(s) g_{f_0\pi^+\pi^-}] + g^{(0)}_{f_0\gamma\gamma}[D_\sigma(s) g_{f_0\pi^+\pi^-} + \Pi_{f_0\sigma}(s) g_{\sigma\pi^+\pi^-}]}{D_\sigma(s) D_{f_0}(s) - \Pi^2_{f_0\sigma}(s)}. \tag{15}$$

To the right-hand side of Eq. (2), we also add the amplitude $M_{\rm res}^{\rm direct}(\gamma\gamma \to \pi^0\pi^0; s) = M_{\rm res}^{\rm direct}(\gamma\gamma \to \pi^+\pi^-; s)$. The factor s in Eq. (15) is due to gauge invariance. The above amplitude also satisfies the unitarity condition. For $\sqrt{s} < 2m_K$, its phase coincides with the $I = 0$ S wave $\pi\pi$ phase shift $\delta_0^0(s) = \delta_B^{\pi\pi}(s) + \delta_{\rm res}(s)$.

Of the existing data, only the Belle ones on the reaction $\gamma\gamma \to \pi^+\pi^-$ in the vicinity of the $f_0(980)$ [Fig. 1(c)] and the Crystal Ball data on the reaction $\gamma\gamma \to \pi^0\pi^0$ for $2m_\pi < \sqrt{s} < 0.8$ GeV [Fig. 1(d)] may be sensitive to the coupling constants $g^{(0)}_{\sigma\gamma\gamma}$ and $g^{(0)}_{f_0\gamma\gamma}$. Therefore, to estimate $g^{(0)}_{\sigma\gamma\gamma}$ and $g^{(0)}_{f_0\gamma\gamma}$ we perform a simultaneous fit to the Crystal Ball data in the above region of $\sqrt{s}$ and the Belle data for $0.85 < \sqrt{s} < 1.15$ GeV. Inclusion of the $\gamma\gamma \to \pi^+\pi^-$ data from a sufficiently wide region around the narrow $f_0(980)$ resonance in the fit is dictated by the following circumstance. The $f_0(980)$ peak is observed in the total cross section $\sigma(\gamma\gamma \to \pi^+\pi^-; |\cos\theta| \le 0.6) = \sigma_0 + \sigma_2$ under the very large, noncoherent, smooth background caused by the contribution of the cross section with $\lambda = 2$, i.e., $\sigma_2 = \sigma_{\lambda=2}(\gamma\gamma \to \pi^+\pi^-, |\cos\theta| \le 0.6)$. It is natural that the $\sqrt{s}$ dependence of this background in the $f_0(980)$ region can be fixed more or less reliably only with the use of the data outside this region. Certainly, σ_2 is dominated by the Born and $f_2(1270)$ resonance contributions. However, first we use a purely phenomenological approximation of σ_2 with a 4th order polynomial in $\sqrt{s}$ in the region $0.85 < \sqrt{s} < 1.15$ GeV. In addition, to obtain a correct fit to the Belle data having the finest step in $\sqrt{s}$, we allow the $f_0(980)$ resonance mass, m_{f_0}, to be a free parameter. We fix the values of the other parameters in the strong amplitudes in accordance with fit 1 from Ref. [13].

Such a fit gives, in remarkable agreement with the prediction of Ref. [9], the negligible values of the direct coupling constants $g^{(0)}_{\sigma\gamma\gamma}$ and $g^{(0)}_{f_0\gamma\gamma}$: $\Gamma^{(0)}_{\sigma\to\gamma\gamma}(m_\sigma^2) = |m_\sigma^2 g^{(0)}_{\sigma\gamma\gamma}|^2/(16\pi m_\sigma) = 0.005$ keV and $\Gamma^{(0)}_{f_0\to\gamma\gamma}(m_{f_0}^2) = |m_{f_0}^2 g^{(0)}_{f_0\gamma\gamma}|^2/(16\pi m_{f_0}) = 0.000\,07$ keV; here $m_{f_0} = 0.972$ GeV [27]. Note, for comparison, that according to estimates presented in Refs. [10,14] the $\sigma(600) \to \gamma\gamma$ decay width via the $\pi^+\pi^-$ loop mechanism is of about 1–2 keV for $0.4 < \sqrt{s} < 0.5$ GeV [14], and the $f_0(980) \to \gamma\gamma$ decay width via the K^+K^- loop mechanism, averaged by the $f_0(980)$ resonance mass distribution in the $\pi\pi$ channel, is of about 0.15–0.2 keV [10]. The results of fitting the Belle data are shown in Figs. 2(a) and 2(b). For comparison, Figs. 2(c) and 2(d) demonstrate the curves corresponding to the fit in which the Crystal Ball data are not taken into account and $g^{(0)}_{\sigma\gamma\gamma} = 0$. In this case, $\Gamma^{(0)}_{f_0\to\gamma\gamma}(m_{f_0}^2) = 0.002$ keV and $m_{f_0} = 0.97$ GeV. The fits to the Belle data for $g^{(0)}_{\sigma\gamma\gamma} = g^{(0)}_{f_0\gamma\gamma} = 0$ are shown in Figs. 2(e) and 2(f); here $m_{f_0} = 0.97$ GeV. Corresponding curves describing the Crystal Ball data in the region $2m_\pi < \sqrt{s} < 0.8$ GeV are not shown because, for the above three variants, they practically coincide with each other and with the curve in Fig. 1(d).

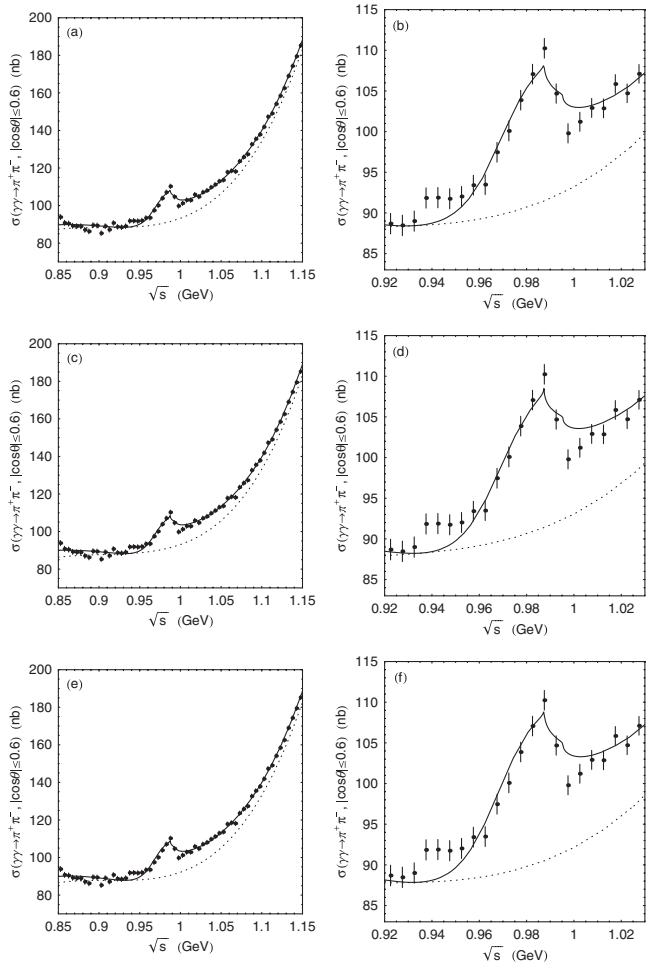

FIG. 2. The results of the three fits pertaining to the Belle data in the vicinity of the $f_0(980)$. They show that the direct couplings of the $\sigma(600)$ and $f_0(980)$ resonances to $\gamma\gamma$ are small. The solid and dotted curves correspond to the cross sections $\sigma(\gamma\gamma \to \pi^+\pi^-; |\cos\theta| \le 0.6) = \sigma_0 + \sigma_2$ and σ_2, respectively. The right-hand plots emphasize the region of the $f_0(980)$ peak. See the text for details.

Thus, the available data on $\gamma\gamma \to \pi\pi$ tell us that the direct couplings of the $\sigma(600)$ and $f_0(980)$ to $\gamma\gamma$ seem to be very small and that the $\sigma(600) \to \gamma\gamma$ and $f_0(980) \to \gamma\gamma$ decays are in fact the four-quark transitions, because they are totally dominated by the $\pi^+\pi^-$ and K^+K^- loop mechanisms, respectively.

To gain a complete understanding of the $f_0(980)$ production mechanism in our model, we present in Figs. 3(a)–3(c) all the main components shaping the $f_0(980)$ signal in σ_0 [see Eqs. (5) and (6)] using the fit shown in Figs. 2(a) and 2(b). Above all, we note that all the curves plotted in Figs. 3(a) and 3(b) correspond to the different contributions to σ_0 from the first term in the curly brackets in Eq. (5), $Z_0|\tilde{A}_S(s)|^2$ with $Z_0 = 0.6$, that is, only from the contributions caused by the final-state interactions. The resulting picture involving the Born and direct $\gamma\gamma$ resonance decay contributions [see Eqs. (1), (5), (6), and (15)] is depicted in Fig. 3(c).

The crucial contribution from the $\gamma\gamma \to K^+K^- \to \pi^+\pi^-$ transition amplitude, $\tilde{A}_S(s) = 8\alpha I_{K^+K^-}(s) \times T_{K^+K^- \to \pi^+\pi^-}(s)$ [see Eqs. (1), (12), and (14)], to σ_0 is shown by the solid curve in Fig. 3(a). This contribution provides the natural scale of the resonance structure in σ_0 in the 1 GeV region. The other curves in the figure represent its constituents. The dashed (dot-dashed) curve corresponds to the contribution from the last (first) two terms in the numerator of Eq. (14) for $T^{K^+K^- \to \pi^+\pi^-}_{\rm res}(s)$, i.e., only from the f_0 (σ) production in the K^+K^- channel; see Ref. [28]. The dotted curve corresponds to the contributions from the last term in the numerator of Eq. (14), i.e., from the $K^+K^- \to f_0 \to \sigma \to \pi^+\pi^-$ transition amplitude caused by the $f_0 - \sigma$ mixing.

The dotted curve in Fig. 3(b) shows the contribution to σ_0 from $\tilde{A}_S(s) = 8\alpha I_{\pi^+\pi^-}(s) e^{2i\delta^{\pi\pi}_B(s)} 2T^{\pi\pi}_{\rm res}(s)/3$, i.e., from the S wave resonance part of the $\gamma\gamma \to \pi^+\pi^- \to \pi^+\pi^-$ transition amplitude [see Eqs. (1), (5), (6), (8), (11), and (13)]. The dot-dashed curve in Fig. 3(b) corresponds to the contribution from $\tilde{A}_S(s) = 8\alpha I_{\pi^+\pi^-}(s) T_{\pi^+\pi^- \to \pi^+\pi^-}(s)$, i. e., from the full S wave $\gamma\gamma \to \pi^+\pi^- \to \pi^+\pi^-$ transition amplitude [see also Eqs. (1), (5), (6), (8), (11), and (13)]. As for the dashed curve in Fig. 3(b), it is identical to the solid one in Fig. 3(a) and is shown for direct comparison of the $\gamma\gamma \to K^+K^- \to \pi^+\pi^-$ and $\gamma\gamma \to \pi^+\pi^- \to \pi^+\pi^-$ contributions. Finally, the solid curve in Fig. 3(b) shows

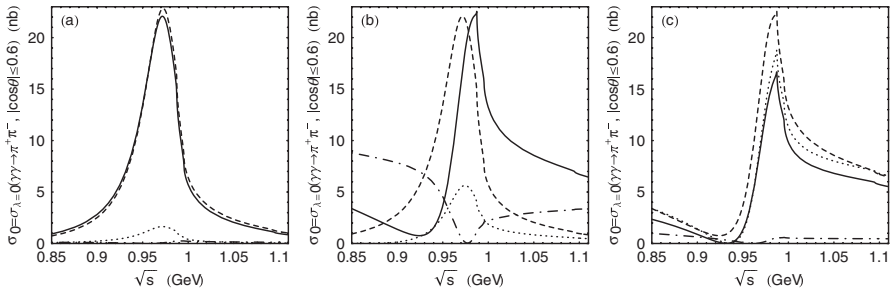

FIG. 3. The main components shaping the $f_0(980)$ signal in σ_0. The contributions from the $\gamma\gamma \to K^+K^- \to \pi^+\pi^-$ and $\gamma\gamma \to \pi^+\pi^- \to \pi^+\pi^-$ transition amplitudes and from the Born and direct $\gamma\gamma$ resonance decay amplitudes are presented. The detailed description of the plotted curves is given in the text.

the total contribution to σ_0 from the $\gamma\gamma \to K^+K^- \to \pi^+\pi^-$ and $\gamma\gamma \to \pi^+\pi^- \to \pi^+\pi^-$ rescattering amplitudes, $\tilde{A}_S(s) = 8\alpha I_{K^+K^-}(s) T_{K^+K^- \to \pi^+\pi^-}(s) + 8\alpha I_{\pi^+\pi^-}(s) \times T_{\pi^+\pi^- \to \pi^+\pi^-}(s)$. A comparison of the dashed, dot-dashed, and solid curves in the figure gives a good idea of the important role of the interference between the background and resonance contributions.

The dashed curve in Fig. 3(c) shows the total contribution to σ_0 from the $\gamma\gamma \to K^+K^- \to \pi^+\pi^-$ and $\gamma\gamma \to \pi^+\pi^- \to \pi^+\pi^-$ rescattering amplitudes; i.e., it is identical to the solid curve in Fig. 3(b). The dotted curve in Fig. 3 (c) corresponds to the contribution from the above rescattering amplitudes plus the Born contributions [see Eqs. (1), (5), and (6)], and the solid curve in the figure represents the resulting picture of the $f_0(980)$ resonance manifestation in $\gamma\gamma \to \pi^+\pi^-$, taking into account the contribution from the direct $\sigma(600) \to \gamma\gamma$ and $f_0(980) \to \gamma\gamma$ decays; see Eq. (15) and also Ref. [29].

We finish this section with a general comment. As already emphasized in Ref. [14], the complex residues of the σ pole in the $\pi\pi \to \pi\pi$ and $\gamma\gamma \to \pi\pi$ amplitudes, used to estimate the $\sigma \to \gamma\gamma$ decay width [21], do not give us an idea about the nature of the σ meson. Furthermore, as noted in Ref. [12], the majority of current investigations of the mass spectra in scalar channels do not study particle production mechanisms. Because of this, such investigations are essentially preprocessing experiments, and the derivable information is very relative. For example, the very first estimate of the σ coupling to the photons via a two-pion intermediate state [30] was restricted to the case of the "bare" (without any background) σ meson, which contradicts the low energy chiral dynamics, and the recent estimates of the $f_0(980) \to \gamma\gamma$ decay width [2,16] have not taken into account the rapidly changing K^+K^- loop production mechanism of the $f_0(980)$ [10]. Nevertheless, the progress in understanding the particle production mechanisms could essentially help us reveal the light scalar meson nature.

V. THE $f_2(1270)$ RESONANCE CONTRIBUTION

To estimate the $f_2(1270) \to \gamma\gamma$ decay width, $\Gamma_{f_2\to\gamma\gamma}(m_{f_2}^2)$, from the data on $\gamma\gamma \to \pi\pi$, it is usually assumed that the $f_2(1270)$ decay occurs mostly into $\gamma\gamma$ states with $\lambda = 2$ [3,4,6,16,19]. For this, the specific models for the background amplitudes with $\lambda = 2$ and 0 are also needed [3,4,6,16,19]. The large background under the $f_2(1270)$ in the $\gamma\gamma \to \pi^+\pi^-$ channel [see, for example, Fig. 1(c)] is dominated by the Born amplitude with $\lambda = 2$. The background situation in the $\gamma\gamma \to \pi^0\pi^0$ channel is more pure. Here, however, uncertainties in the data and bins of $\sqrt{s}$ are still rather large. Different assumptions about the background amplitudes in the $f_2(1270)$ region have been used in the literature [3,4,6,16,19]. In so doing, the central values of $\Gamma_{f_2\to\gamma\gamma}(m_{f_2}^2)$ obtained in the independent experiments lie in the range from 2.3 to 3.6 keV [3,4,6,19,31].

According to the Particle Data Group (PDG) estimate [31], $\Gamma_{f_2\to\gamma\gamma}(m_{f_2}^2) = 2.6 \pm 0.24$ keV. In the recent work [16], the authors of the Belle experiment presented "a consistency check" of their data in the $f_2(1270)$ region with this estimate. They fixed the values of the $f_2(1270)$ resonance parameters as given by the PDG [31] and, using a simple phenomenological parametrization of the background amplitudes, performed the fit to the data on $\sigma(\gamma\gamma \to \pi^+\pi^-; |\cos\theta| \le 0.6)$ in the region $m_{f_2} - \Gamma_{f_2}^{\rm tot} \le \sqrt{s} \le m_{f_2} + \Gamma_{f_2}^{\rm tot}$, i.e., for $1.090 \le \sqrt{s} \le 1.461$ GeV. The resulting fit turned out to be very good, and they concluded that the "consistency check is satisfactory." Unfortunately, in Ref. [16] the factor $\sqrt{2/3}$ has been missed in the $f_2(1270)$ production amplitude in Eq. (10). Thus, the consistency is broken. In fact, it follows from the Belle data [16] that $\Gamma_{f_2\to\gamma\gamma}(m_{f_2}^2) \approx 3.9$ keV, which is 1.5 times greater than the PDG estimate. At the same time, this value is in close agreement with our estimate, $\Gamma_{f_2\to\gamma\gamma}(m_{f_2}^2) \approx 3.8$ keV, which we obtained from the Belle data, but in another way (see below).

To describe the Belle data in the region $0.8 \le \sqrt{s} \le 1.5$ GeV, we use the expression for the total cross section $\sigma(\gamma\gamma \to \pi^+\pi^-; |\cos\theta| \le 0.6) = \sigma_0 + \sigma_2$. The cross section σ_0 has been constructed in Secs. III and IV, and the cross section σ_2 involving the Born and $f_2(1270)$ resonance contributions has the form [18,19]

$$\sigma_2 = \frac{8\pi}{s}\int_0^{0.6} \left| \frac{\sqrt{\rho_{\pi^+}(s)}}{16\pi} M_2^{\rm Born}(s,\theta) + 5 d_{20}^2(\theta) \times \frac{\sqrt{s} G_2(s) \sqrt{2\Gamma_{f_2\to\pi\pi}(s)/3}}{m_{f_2}^2 - s - i\sqrt{s}\Gamma_{f_2}^{\rm tot}(s)} \right|^2 d\cos\theta, \quad (16)$$

where $M_2^{\rm Born}(s,\theta) = 8\pi\alpha\rho_{\pi^+}^2(s)\sin^2\theta/[1 - \rho_{\pi^+}^2(s)\cos^2\theta]$ is the Born helicity-2 amplitude $\gamma\gamma \to \pi^+\pi^-$, $d_{20}^2(\theta) = \frac{\sqrt{6}}{4}\sin^2\theta$, and the energy-dependent total width of the $f_2(1270)$ is given by $\Gamma_{f_2}^{\rm tot}(s) = \Gamma_{f_2\to\pi\pi}(s) + \Gamma_{f_2\to K\bar{K}}(s) + \Gamma_{f_2\to 4\pi}(s)$. The partial width $\Gamma_{f_2\to\pi\pi}(s)$ is parametrized as [3]

$$\Gamma_{f_2\to\pi\pi}(s) = \Gamma_{f_2}^{\rm tot}(m_{f_2}^2) B(f_2 \to \pi\pi) \frac{m_{f_2}^2}{s} \times \frac{q_{\pi^+}^5(s)}{q_{\pi^+}^5(m_{f_2}^2)} \frac{D_2(q_{\pi^+}(s) R_{f_2})}{D_2(q_{\pi^+}(m_{f_2}^2) R_{f_2})}, \quad (17)$$

where $D_2(x) = 1/(9 + 3x^2 + x^4)$, $q_{\pi^+}(s) = \sqrt{s}\rho_{\pi^+}(s)/2$, and R_{f_2} is an interaction radius. $\Gamma_{f_2\to K\bar{K}}(s)$ has the form similar to Eq. (17), and $\Gamma_{f_2\to 4\pi}(s)$ as a function of s is approximated by the S wave $f_2(1270) \to \rho\rho \to 4\pi$ decay width; see, for example, Ref. [9]. The branching ratios are $B(f_2 \to \pi\pi) = 0.847$, $B(f_2 \to K\bar{K}) = 0.046$, and $B(f_2 \to 4\pi) = 0.107$ [31]. Finally,

$$G_2(s) = \sqrt{\Gamma^{(0)}_{f_2\to\gamma\gamma}(s)} + i\frac{\sqrt{\rho_{\pi^+}(s)}}{16\pi}M^{\rm Born}_{22}(s) \times\sqrt{2\Gamma_{f_2\to\pi\pi}(s)/3}. \quad (18)$$

By definition, $\Gamma_{f_2\to\gamma\gamma}(s) = |G_2(s)|^2$. For $\Gamma^{(0)}_{f_2\to\gamma\gamma}(s)$ we use the following parametrization:

$$\Gamma^{(0)}_{f_2\to\gamma\gamma}(s) = \frac{m_{f_2}}{\sqrt{s}}\Gamma^{(0)}_{f_2\to\gamma\gamma}(m^2_{f_2})\left(\frac{s^2}{m^4_{f_2}}\frac{m^2_{f_2}+\Lambda^2_{f_2}}{s+\Lambda^2_{f_2}}\right)^2. \quad (19)$$

The second term in Eq. (18) corresponds to the four-quark transition of the $f_2(1270)$ into photons via the $\pi^+\pi^-$ real intermediate state, $f_2(1270)\to\pi^+\pi^-\to\gamma\gamma$, where

$$M^{\rm Born}_{22}(s) = 4\pi\alpha\sqrt{\frac{3}{2}}\left[\frac{1-\rho^2_{\pi^+}(s)}{2\rho^3_{\pi^+}(s)}\ln\frac{1+\rho_{\pi^+}(s)}{1-\rho_{\pi^+}(s)} - \frac{1}{\rho^2_{\pi^+}(s)} + \frac{5}{3}\right] \quad (20)$$

is the Born partial, helicity amplitude $\gamma\gamma\to\pi^+\pi^-$ with $J=\lambda=2$. This term ensures the fulfilment of the Watson theorem requirement for the $I=0$, $J=\lambda=2$ amplitude $\gamma\gamma\to\pi\pi$ in the elastic region. It gives a rather small contribution to $\Gamma_{f_2\to\gamma\gamma}(m^2_{f_2})$:

$$\Gamma_{f_2\to\gamma\gamma}(m^2_{f_2}) = \Gamma^{(0)}_{f_2\to\gamma\gamma}(m^2_{f_2}) + 0.21\ \text{keV}. \quad (21)$$

It is generally accepted that the $f_2(1270)\to\gamma\gamma$ decay rate is dominated by the direct quark-antiquark transition $q\bar{q}\to\gamma\gamma$, that is, by $\Gamma^{(0)}_{f_2\to\gamma\gamma}(m^2_{f_2})$. As we saw above, for the lightest scalar mesons, the situation is reversed.

In the fit, we use as free parameters $\Gamma^{(0)}_{f_2\to\gamma\gamma}(m_{f_2})$, m_{f_2}, $\Gamma^{\rm tot}_{f_2}(m^2_{f_2})$, R_{f_2}, Λ_{f_2}, and also $g^{(0)}_{\sigma\gamma\gamma}$, $g^{(0)}_{f_0\gamma\gamma}$, and m_{f_0}. The parameters R_{f_2} and Λ_{f_2} control the s dependencies of the $f_2(1270)$ partial decay widths, and consequently, they are responsible for the shape of the $f_2(1270)$ line. The results of the fit to the Belle data are shown in Figs. 4(a)–4(c). Figure 4(a) demonstrates the overall picture of the most important contributions in the region $2m_\pi \le \sqrt{s} \le 1.5$ GeV; here σ_{f_2} is the cross section corresponding to the $f_2(1270)$ resonance contribution and the dotted curve shows the contribution of the interference between the $f_2(1270)$ and background amplitudes in σ_2. The descriptions of the Belle data in the whole investigated region of $\sqrt{s}$ and in the $f_0(980)$ resonance region are presented in more detail in Figs. 4(b) and 4(c), respectively. The parameters obtained are $\Gamma^{(0)}_{f_2\to\gamma\gamma}(m_{f_2}) = 3.59$ keV [$\Gamma_{f_2\to\gamma\gamma}(m_{f_2}) = 3.8$ keV, see Eq. (21)], $m_{f_2} = 1.279$ GeV, $\Gamma^{\rm tot}_{f_2}(m^2_{f_2}) = 0.188$ GeV, $R_{f_2} = 2.575$ GeV^{-1}, $\Lambda_{f_2} = 3.52$ GeV, $g^{(0)}_{\sigma\gamma\gamma} = 0.482$ GeV^{-1} [$\Gamma^{(0)}_{\sigma\to\gamma\gamma}(m^2_\sigma) = 0.01$ keV], $g^{(0)}_{f_0\gamma\gamma} = -0.867$ GeV^{-1} [$\Gamma^{(0)}_{f_0\to\gamma\gamma}(m^2_{f_0}) = 0.015$ keV], and $m_{f_0} = 0.975$ GeV. Because of the smallness of statistical uncertainties in the Belle data, the formally calculated errors of the above-listed parameters turn out to be negligible. In similar situations, the model dependence of the fitted parameter values is the most important source of their uncertainty.

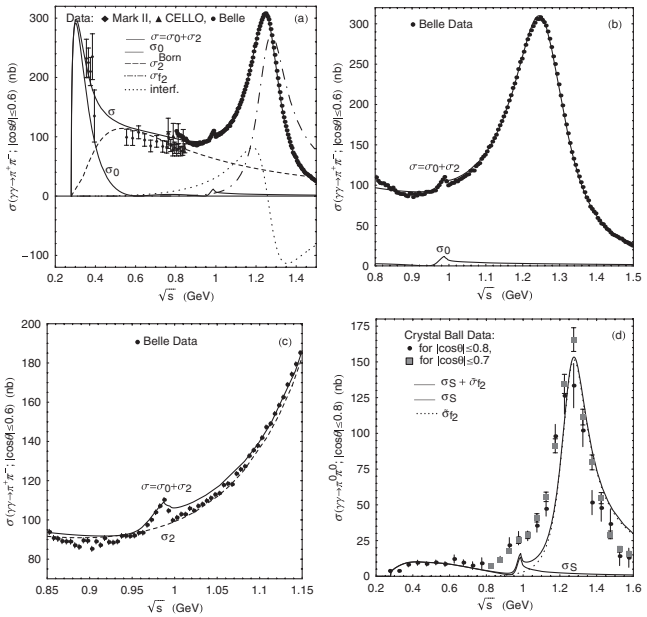

FIG. 4. The fit to the Belle data on the $\gamma\gamma\to\pi^+\pi^-$ cross section and the comparison with the Crystal Ball data on the $\gamma\gamma\to\pi^0\pi^0$ cross section. See the text for details.

The obtained description of the Belle data as a whole seems to be quite satisfactory, except for minor details [32]. The more important result of the fit is that the values of the direct coupling constants of the $\sigma(600)$ and $f_0(980)$ resonances to $\gamma\gamma$ turn out to be small (see the above-mentioned corresponding decay widths). Of course, the obtained concrete values of these constants are, evidently, rather conditional (compare, for example, the above fitting variant with that presented in Sec. IV). Let us stress, however, that the very fact of the suppression of the direct $\sigma(600)$ and $f_0(980)$ couplings to photons (corresponding widths are much less than 1 keV) can be considered to be well established. In addition, it appears from the new Belle data that $\Gamma_{f_2\to\gamma\gamma}(m_{f_2})$ is about a factor of 1.5 higher than the estimate quoted by the PDG [31].

We now construct the $\gamma\gamma\to\pi^0\pi^0$ reaction cross section $\sigma(\gamma\gamma\to\pi^0\pi^0; |\cos\theta| \le 0.8) = \sigma_S + \tilde{\sigma}_{f_2}$, where $\tilde{\sigma}_{f_2}$ is the $f_2(1270)$ production cross section in the $\pi^0\pi^0$ channel (an analog of σ_{f_2} for the $\pi^+\pi^-$ one), and compare it with the Crystal Ball data [3,7]. The result is shown in Fig. 4(d). As is seen, the agreement with the data is very poor in the whole region of the $f_2(1270)$ resonance influence, i.e., for $\sqrt{s}$ from 0.8 to 1.6 GeV. We verified that the parametrization of the $f_2(1270)$ contribution used by the Belle Collaboration [16] leads to a similar resonance pattern. To improve the description of the available data on the

reaction $\gamma\gamma \to \pi^0\pi^0$, it is necessary to raise the left wing of the $f_2(1270)$ resonance and to lower its right one [33], i. e., to change the $f_2(1270)$ resonance shape in comparison with that established from the $\gamma\gamma \to \pi^+\pi^-$ data.

As for the above difficulty, in fact, it arose as the first detailed experiments were carried out on the reactions $\gamma\gamma \to \pi^0\pi^0$ [3,7] and $\gamma\gamma \to \pi^+\pi^-$ [4,6]. Different parametrizations of the $f_2(1270)$ resonance shape have been used in Refs. [3,4,6]. Taking the corresponding formulas and fitting parameters from Refs. [3,4,6], we have made sure that in the early analyses [3,4,6] the appreciably different shapes of the $f_2(1270)$ peak in the $\pi^0\pi^0$ and $\pi^+\pi^-$ channels were obtained. The difference bears the above-mentioned character. However, the existing uncertainties in the Crystal Ball [3,7], Mark II [4], and CELLO [6] data [see, for example, Figs. 1(a) and 1(d)] hamper any definite conclusions about their possible inconsistency or about the urgent need for searching the additional mechanisms to obtain a good simultaneous description of the $\pi^0\pi^0$ and $\pi^+\pi^-$ data in the $f_2(1270)$ region. It is clear that the Belle experiment on the reaction $\gamma\gamma \to \pi^+\pi^-$ [2,16] essentially aggravates the situation because its results are based on statistics which are about 3 orders of magnitude higher than those collected in the Crystal Ball experiments. So, it is clear that, in the first place, very high quality data on the reaction $\gamma\gamma \to \pi^0\pi^0$ and their partial wave analysis would be extremely useful to obtain reliable conclusions from the simultaneous description of the $\pi^+\pi^-$ and $\pi^0\pi^0$ channels [34].

After this work was completed, very high statistics Belle data on the reaction $\gamma\gamma \to \pi^0\pi^0$ for $\sqrt{s} > 0.6$ GeV [37] appeared, which are in close agreement with the Crystal Ball measurements [3,7]. Probably, this implies that a damping form factor [34] in the $\gamma\gamma \to \pi^+\pi^-$ Born amplitudes is really needed for the simultaneous description of the $\pi^+\pi^-$ and $\pi^0\pi^0$ production cross sections in the $f_2(1270)$ resonance region. Such an investigation requires considerable efforts, because the form factor influence should be taken into account in partial waves and in loop contributions. We shall present a careful analysis of the compatibility of the new $\gamma\gamma \to \pi^+\pi^-$ and $\gamma\gamma \to \pi^0\pi^0$ data from Belle elsewhere, together with comments on the choice of a suitable phenomenological form factor. Here we only announce some preliminary results of our analysis.

New high statistics results from Belle on the $\gamma\gamma \to \pi^0\pi^0$ reaction cross section [37] are shown in Fig. 5. In spite of very small statistical errors [37], these data can be quite satisfactorily described [33], separately from the data for the $\gamma\gamma \to \pi^+\pi^-$ production; see, as an example, the solid curve in Fig. 5(b) which corresponds to the parameters $\Gamma^{(0)}_{f_2\to\gamma\gamma}(m_{f_2}) = 3.24$ keV [$\Gamma_{f_2\to\gamma\gamma}(m_{f_2}) = 3.43$ keV], $m_{f_2} = 1.272$ GeV, $\Gamma^{\rm tot}_{f_2}(m^2_{f_2}) = 0.183$ GeV, $R_{f_2} = 6.5$ GeV^{-1}, $\Lambda_{f_2} = 0$, $g^{(0)}_{\sigma\gamma\gamma} = 0.542$ GeV^{-1}, $g^{(0)}_{f_0\gamma\gamma} = 0.468$ GeV^{-1}, and $m_{f_0} = 0.969$ GeV. However, such a fit to the $\gamma\gamma \to \pi^0\pi^0$ cross section is in apparent contradiction with the $\gamma\gamma \to \pi^+\pi^-$ data; see the solid curve for $\sigma = \sigma_0 + \sigma_2$ in Fig. 5(a). This is caused mainly by the large Born contributions to σ_2 in the $\gamma\gamma \to \pi^+\pi^-$ channel. Recall that such contributions are absent in $\gamma\gamma \to \pi^0\pi^0$. Thus, the situation can be essentially improved by multiplying the $\gamma\gamma \to \pi^+\pi^-$ Born amplitudes by some overall, damping form factor $G(t, u)$ [34,35], where t and u are the usual Mandelstam variables for the reaction $\gamma\gamma \to \pi^+\pi^-$. For this we use here the expression proposed by Poppe [35],

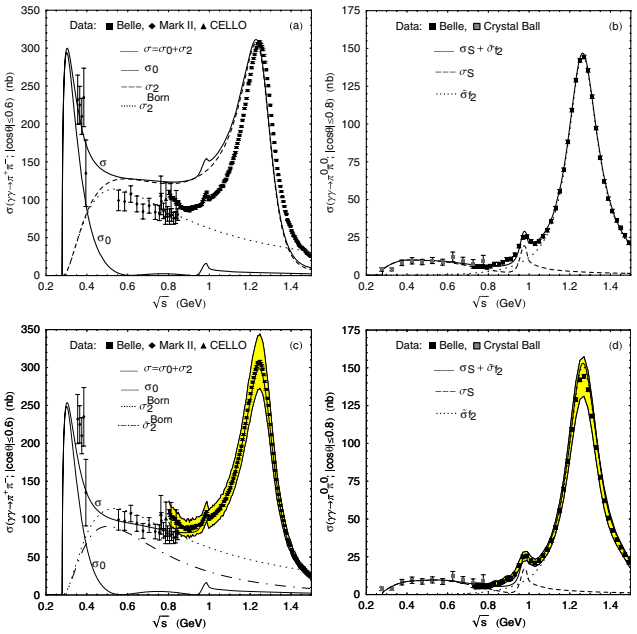

FIG. 5 (color online). An illustration of the simultaneous description of the new high statistics Belle data on the $\gamma\gamma \to \pi^+\pi^-$ [2,16] and $\gamma\gamma \to \pi^0\pi^0$ [37] reaction cross sections. The Belle data in plots (a), (b), (c), and (d) are represented by full squares with statistical error bars. The shaded bands in (c) and (d) correspond to the Belle data taking into account their systematic errors [2,16,37]. The curves in (b) and (a) correspond to the fit to the $\gamma\gamma \to \pi^0\pi^0$ data and its consequence for the $\gamma\gamma \to \pi^+\pi^-$ channel, respectively. The curves in (c) and (d) correspond to the overall fit to the $\gamma\gamma \to \pi^+\pi^-$ and $\gamma\gamma \to \pi^0\pi^0$ data in the regions $0.85 < \sqrt{s} < 1.5$ GeV and $2m_\pi < \sqrt{s} < 1.5$ GeV, respectively, in the model with a form factor. $\tilde{\sigma}_2^{\rm Born}$ in (c) is the $\lambda = 2$ Born cross section modified by a form factor. See the text for details.

$$G(t,u) = -\frac{1}{s}\left[\frac{t - m^2_{\pi^+}}{1 - (u - m^2_{\pi^+})/x_1^2} + \frac{u - m^2_{\pi^+}}{1 - (t - m^2_{\pi^+})/x_1^2}\right],$$

where x_1 is a free parameter. This ansatz is quite acceptable in the physical region of the reaction $\gamma\gamma \to \pi^+\pi^-$. Replacing m_{π^+} and x_1 by m_{K^+} and x_2, respectively, we also obtain a form factor suitable for the $\gamma\gamma \to K^+K^-$ Born amplitude. The solid curves for $\sigma = \sigma_0 + \sigma_2$ and $\sigma_S + \tilde{\sigma}_{f_2}$ in Figs. 5(c) and 5(d), respectively, show an

example of the overall fit to the new $\gamma\gamma \to \pi^+\pi^-$ and $\gamma\gamma \to \pi^0\pi^0$ data, taking into account the form factors modifying the Born contributions. The obtained description is quite reasonable (if not excellent), but only within systematic errors of the data, which are plotted in Figs. 5(c) and 5(d) in the form of the shaded bands. We think that such a treatment of the high statistics Belle data is sufficiently justified. Statistical errors of the two Belle measurements are so small that obtaining the formally acceptable χ^2 for simultaneous fits to the data is practically impossible. The curves in Figs. 5(c) and 5(d) correspond to the parameters $\Gamma^{(0)}_{f_2\to\gamma\gamma}(m_{f_2}) = 3.60$ keV [$\Gamma_{f_2\to\gamma\gamma}(m_{f_2}) = 3.68$ keV; we consider this estimate for $\Gamma_{f_2\to\gamma\gamma}(m_{f_2})$ as the most preferable one], $m_{f_2} = 1.272$ GeV, $\Gamma^{\rm tot}_{f_2}(m^2_{f_2}) = 0.188$ GeV, $R_{f_2} = 5$ GeV^{-1}, $\Lambda_{f_2} = 0$, $g^{(0)}_{\sigma\gamma\gamma} = g^{(0)}_{f_0\gamma\gamma} = 0$, $m_{f_0} = 0.969$ GeV, $x_1 = 1$ GeV, and $x_2 = 3$ GeV. A comparison of Figs. 5(b) and 5(d) shows that the impact of the form factor on the $\gamma\gamma \to \pi^0\pi^0$ cross section turns out to be really small, in contrast to the case of the $\gamma\gamma \to \pi^+\pi^-$ production; see Figs. 5(a) and 5(c). Note also that all the above conclusions about the production mechanisms of the $\sigma(600)$ and $f_0(980)$ resonances and a comment on the angular distribution for the nonresonance background, given in Sec. II, remain valid.

VI. CONCLUSION

We have analyzed the new high statistics Belle data on the reaction $\gamma\gamma \to \pi^+\pi^-$ taking into account its main dynamical mechanisms. The analysis has shown that the direct coupling constants of the $\sigma(600)$ and $f_0(980)$ resonances to $\gamma\gamma$ are small, which is typical [9] for the four-quark nature [38] of these states. Our main conclusion is that the $\sigma(600) \to \gamma\gamma$ and $f_0(980) \to \gamma\gamma$ decays are the four-quark transitions that are dominated mainly by the $\pi^+\pi^-$ and K^+K^- loop mechanisms, respectively. In addition, we have presented some results of a simultaneous description of the $\gamma\gamma \to \pi^+\pi^-$ data and the latest, very high statistics Belle data on the reaction $\gamma\gamma \to \pi^0\pi^0$. We have also estimated the $f_2(1270) \to \gamma\gamma$ decay width. We intend to develop the above analysis to further understand the light scalar meson physics.

ACKNOWLEDGMENTS

We thank Y. Watanabe very much for communication and for the table with the Belle data for $\gamma\gamma \to \pi^+\pi^-$. This work was supported in part by the Presidential Grant No. NSh-5362.2006.2 for Leading Scientific Schools and by the RFFI Grant No. 07-02-00093 from the Russian Foundation for Basic Research.

[1] T. Mori *et al.* (Belle Collaboration), in *Proceedings of the International Symposium on Hadron Spectroscopy Chiral Symmetry and Relativistic Description of Bound Systems, Tokyo, 2003*, edited by S. Ishida, K. Takamatsu, T. Tsuru, S. Y. Tsai, M. Ishida, and T. Komada (KEK, Tsukuba, 2003), p. 159.
[2] T. Mori *et al.* (Belle Collaboration), Phys. Rev. D **75**, 051101 (2007).
[3] H. Marsiske *et al.*, Phys. Rev. D **41**, 3324 (1990).
[4] J. Boyer *et al.*, Phys. Rev. D **42**, 1350 (1990).
[5] T. Oest *et al.*, Z. Phys. C **47**, 343 (1990).
[6] H. J. Behrend *et al.*, Z. Phys. C **56**, 381 (1992).
[7] J. K. Bienlein, in *Proceedings of the IX International Workshop on Photon-Photon Collisions, San Diego, 1992*, edited by D. Caldwell and H. P. Paar (*World Scientific*, Singapore, 1992), p. 241.
[8] R. Barate *et al.*, Phys. Lett. B **472**, 189 (2000).
[9] N. N. Achasov, S. A. Devyanin, and G. N. Shestakov, Phys. Lett. **108B**, 134 (1982); Z. Phys. C **16**, 55 (1982).
[10] N. N. Achasov and G. N. Shestakov, Phys. Rev. D **72**, 013006 (2005); Yad. Fiz. **69**, 1545 (2006) Phys. At. Nucl. **69**, 1510 (2006).
[11] N. N. Achasov, A. V. Kiselev, and G. N. Shestakov, Nucl. Phys. B, Proc. Suppl. **162**, 127 (2006).
[12] N. N. Achasov, in *Proceedings of the 14th International Seminar QUARKS-2006, Repino, St. Peterburg, 2006*, edited by S. V. Demidov, V. A. Matveev, V. A. Rubakov, and G. I. Rubtsov (INR RAS, Moscow, 2007), p. 37; arXiv:hep-ph/0609261.
[13] N. N. Achasov and A. V. Kiselev, Phys. Rev. D **73**, 054029 (2006).
[14] N. N. Achasov and G. N. Shestakov, Phys. Rev. Lett. **99**, 072001 (2007); arXiv:0704.2368.
[15] N. N. Achasov and G. N. Shestakov, Phys. Rev. D **49**, 5779 (1994); Yad. Fiz. **56**, No. 9, 206 (1993) Phys. At. Nucl. **56**, 1270 (1993).
[16] T. Mori *et al.* (Belle Collaboration), J. Phys. Soc. Jpn. **76**, 074102 (2007); arXiv:0704.3538.
[17] G. Mennessier, Z. Phys. C **16**, 241 (1983).
[18] D. H. Lyth, J. Phys. G **11**, 459 (1985).
[19] R. P. Johnson, Ph.D. thesis [SLAC Report No.-294, 1986 (unpublished)].
[20] D. Morgan and M. R. Pennington, Phys. Lett. B **192**, 207 (1987); Z. Phys. C **37**, 431 (1988); Phys. Lett. B **272**, 134 (1991).
[21] M. R. Pennington, Phys. Rev. Lett. **97**, 011601 (2006).
[22] N. N. Achasov and V. V. Gubin, Phys. Rev. D **57**, 1987 (1998); Yad. Fiz. **61**, 1473 (1998) Phys. At. Nucl. **61**, 1367 (1998).
[23] The authors of Refs. [1,2,16] erroneously believe that the Flatte work [39] is related to the formula that they have used in their works for the $f_0(980)$ propagator $1/D_{f_0}(s)$. This formula for $1/D_{f_0}(s)$ was first obtained in Ref. [40].
[24] There is a misprint in this fit in the sign of the constant

$C \equiv C_{f_0\sigma}$; here we use $C_{f_0\sigma} = -0.047$ GeV^2.

[25] N. N. Achasov and G. N. Shestakov, Phys. Rev. D **67**, 114018 (2003); Yad. Fiz. **67**, 1380 (2004) Phys. At. Nucl. **67**, 1355 (2004).

[26] G. Mennessier, P. Minkowski, S. Narison, and W. Ochs, arXiv:0707.4511.

[27] This m_{f_0} value is about 12 MeV smaller than that obtained in fit 1 from Ref. [13], but in so doing the description of the $\pi\pi$ phase shift $\delta_0^0(s)$ essentially does not deteriorate.

[28] This contribution from the σ production is negligible, and in Fig. 3(a) it is increased by a factor of 10.

[29] The contribution from the direct $\gamma\gamma$ resonance decay amplitude $M_{\rm res}^{\rm direct}(\gamma\gamma \to \pi^+\pi^-; s)$ is very small and that is why this is increased by a factor of 10 in Fig. 3(c) (see the corresponding dot-dashed curve). However, as is seen from this figure, the interference between the amplitude $M_{\rm res}^{\rm direct}(\gamma\gamma \to \pi^+\pi^-; s)$ and the main ones is quite noticeable.

[30] P. C. DeCelles and J. F. Goehl, Phys. Rev. **184**, 1617 (1969).

[31] W.-M. Yao *et al.* (Particle Data Group), J. Phys. G **33**, 1 (2006).

[32] In principle, these details [see Figs. 4(b) and 4(c)] can be artifacts associated with the event selection procedure employed. It must be kept in mind that the systematic errors in the Belle experiment are an order of magnitude higher than the statistical ones [1,2,16]. Here we add yet an evident remark. In order to improve the data description, it is necessary to increase the flexibility of the phenomenological model in use. As a rule, this is accompanied both by new assumptions and by introducing additional free parameters.

[33] Formally, this is easy to implement, for example, by increasing R_{f_2} and decreasing Λ_{f_2} and m_{f_2} relative to the $\pi^+\pi^-$ case.

[34] Generally speaking, the consistent description of the Crystal Ball and Belle data could be implemented by introducing a form factor into the Born amplitudes. Such a form factor (see Refs. [4,6,20,35,36] for details) suppresses the continuum in the $f_2(1270)$ region in the $\pi^+\pi^-$ channel and, thus, permits the left wing of the $f_2(1270)$ resonance to be increased in agreement with the available $\pi^+\pi^-$ and $\pi^0\pi^0$ data.

[35] M. Poppe, Int. J. Mod. Phys. A **1**, 545 (1986).

[36] N. N. Achasov and G. N. Shestakov, Mod. Phys. Lett. A **9**, 1351 (1994).

[37] K. Abe *et al.* (Belle Collaboration), arXiv:0711.1926.

[38] R. L. Jaffe, Phys. Rev. D **15**, 267 (1977); **15**, 281 (1977).

[39] S. M. Flatte, Phys. Lett. **63B**, 224 (1976).

[40] N. N. Achasov, S. A. Devyanin, and G. N. Shestakov, Yad. Fiz. **32**, 1098 (1980) [Sov. J. Nucl. Phys. **32**, 566 (1980)].